



## OPEN $\gamma\delta$ T cell distribution in the adventitial layer of non-fertile cystic echinococcosis cysts from cattle livers

Caroll Stoore<sup>1</sup>, María Soledad Baquedano<sup>1</sup>, Christian Hidalgo<sup>2</sup>, Claudio Cabello-Verrugio<sup>3,4</sup> & Rodolfo Paredes<sup>1</sup>✉

Cystic Echinococcosis (CE) is a zoonotic disease caused by *Echinococcus granulosus sensu lato*, forming cysts in ruminants and humans with major health and economic impacts. The immune response to CE cysts is complex, with fertility linked to the host's inflammatory reaction. This study examines  $\gamma\delta$  T cell distribution and role within the adventitial layer of non-fertile CE cysts in cattle, including cases co-infected with the trematode *Fasciola hepatica* (FH), a known immune response modulator. Using immunohistochemistry and double immunofluorescence, we observed  $\gamma\delta$  T cells dispersed in the adventitial layer, enriched in inflammatory zones. Co-infected cases (CE + FH+) showed a reduced  $\gamma\delta$  T cell proportion among CD3+ T cells compared to non-coinfected cases, suggesting an immunoregulatory effect of FH. Our findings align with prior studies showing  $\gamma\delta$  T cell recruitment in granulomatous diseases in ruminants but reveal that co-infection alters this response. This study provides the first detailed characterization of  $\gamma\delta$  T cells in cattle CE cysts, emphasizing their potential role in granulomatous immune responses. It highlights the need for further research into mechanisms influencing CE cyst fertility and immune modulation in helminth co-infections, advancing our understanding of host-pathogen interactions and informing disease management strategies.

**Keywords** Cystic echinococcosis, Adventitial layer, Gamma-delta lymphocytes, Co-infection

Cystic Echinococcosis (CE) is a zoonotic parasitological infection caused by the metacestode of *Echinococcus granulosus sensu lato* (*s.l.*). Recognized by the World Health Organization as a Neglected Tropical Disease (NTD), CE is widespread globally<sup>1</sup>. *Echinococcus granulosus sensu lato* is a species cluster in which *Echinococcus granulosus sensu stricto* (*s.s.*) accounts for most of human and animal CE cases<sup>2–4</sup>. This cestode has an indirect life cycle, with herbivores, such as sheep and cattle, as intermediate hosts and canids as definitive hosts. Humans are considered dead-end hosts. The intermediate and dead-end hosts ingest the oncospheres from canid feces, which then migrate mainly to the host's lungs and liver, where they establish a CE cyst, also known as a hydatid cyst<sup>5</sup>. CE cysts are fluid-filled vesicles with a wall composed of three layers. The germinal layer (GL) and laminated layer (LL) of parasite origin, and the adventitial layer generated by the host immune response. The inner cellular GL produces parasite components such as brood capsules and protoscolices (PSC), the LL, and hydatid cyst fluid<sup>6</sup>. Viable PSCs are infective for the definitive hosts. Some CE cysts do not have PSC, and thus are considered non-fertile, as they are not able to continue with the parasite's life cycle<sup>4</sup>. Regarding the host immune response, T helper 1 (Th1) mediated immune response, which is characterized by inflammatory cytokines like gamma interferon (IFN- $\gamma$ ), is found detrimental to the parasite but a later Th2 immune response is beneficial for the chronic establishment and survival of the parasite; in consequence, maintenance of local inflammation is associated with low parasite viability whereas fibrotic resolution is associated with prosperous metacestodes<sup>7</sup>. The degree of inflammation or development of the adventitial layer is repeatedly found associated with fertility<sup>8,9</sup>. In cattle, non-fertile cysts have thin laminated layers, epithelioid macrophages beneath the laminated layer, lymphoid follicles and multinucleated gigantic cells through the adventitial layer, with little presence of collagen fibers or fibroblasts<sup>8</sup>. The features found in non-fertile CE cysts are hallmarks of a granulomatous immune

<sup>1</sup>Escuela de Medicina Veterinaria, Facultad de Ciencias de la Vida, Universidad Andres Bello, Santiago, Chile.

<sup>2</sup>Núcleo de Investigación en One Health (NIOH), Facultad de Medicina Veterinaria y Agronomía, Universidad de las Américas, Santiago Centro, Chile. <sup>3</sup>Center for Research on Pandemic Resilience, Faculty of Life Science, Universidad Andres Bello, Santiago, Chile. <sup>4</sup>Millennium Institute on Immunology and Immunotherapy, Faculty of Life Sciences, Universidad Andres Bello, Santiago, Chile. ✉email: rparedes@unab.cl

response<sup>10</sup>. Studies of the composition of the cells participating in this granulomatous response, specifically lymphocytes, are necessary to fully understand the molecular mechanisms involved in CE cyst fertility.

Lymphocytes are an important cellular component in the immunologic response to the *Echinococcus granulosus* metacestode<sup>11</sup>. The most frequent type of lymphocyte infiltrating the adventitial layer of human<sup>12</sup>, sheep<sup>13</sup>, and cattle CE cysts are CD3+ T cells<sup>14,15</sup>.

T cells are distinguished based on the presence of an alpha beta ( $\alpha\beta$ ) or a gamma delta ( $\gamma\delta$ ) TCR into  $\alpha\beta$  or  $\gamma\delta$  T cells. In contrast to traditional  $\alpha\beta$  T cells, the majority of  $\gamma\delta$  TCRs do not recognize MHC molecules, which is in line with a lack of CD4 and CD8 expression by most  $\gamma\delta$  T cells<sup>16</sup>. Another particular characteristic of  $\gamma\delta$  T cells is that they also recognize non-peptide antigens, pathogen-associated molecular patterns (PAMPs) or danger-associated molecular patterns (DAMPs), and have both innate and adaptive immune functions<sup>17</sup>.

Information available for subtypes of CD3+ lymphocytes in the adventitial layer of cattle CE cysts is restricted to CD4+ and CD8+ cells<sup>15</sup>. In ruminants,  $\gamma\delta$  T cells constitute a major lymphocyte population in peripheral blood, epithelial tissues, and sites of inflammation. The high frequency of  $\gamma\delta$  T cells in the peripheral blood (constituting 15–60% of peripheral blood mononuclear cells), particularly in young animals, suggests an important role in host defense<sup>18,19</sup>.

Studies on infectious diseases focus on one host and pathogen systems, whereas hosts are typically infected by multiple parasite species<sup>20,21</sup>. In this subject, immunoregulation of helminths to other pathogens is a recognized phenomenon<sup>22,23</sup>. One example is *Fasciola hepatica*, a hepatic parasitic trematode that, like *Echinococcus granulosus*, establishes long lasting chronic infections in its hosts<sup>24</sup>. Previous results show close to 50% of cattle are chronically infected by *F. hepatica*<sup>25</sup>. Extensive data shows that this longevity within the host is due to the ability of *F. hepatica* to modulate the host immune response to benefit its survival and one of these mechanisms is the suppression of Th1/Th17 responses and promotion of a strong Th2/Treg response<sup>21,26,27</sup>. This shift not only affects the immune response to the parasite itself but also alters the response to co-infecting pathogens<sup>28</sup>. Studies of  $\gamma\delta$  T cells in *Fasciola hepatica* infected hosts are few and confounding. One study in primary chronically infected sheep found that  $\gamma\delta$  T cells were a prominent feature in the fibrotic strands<sup>29</sup>. Sheep experimentally infected with *F. hepatica* found that  $\gamma\delta$  T cells subpopulations increased in late-stage infections<sup>30</sup>. No studies are available in the literature that characterize in cattle, the  $\gamma\delta$  T cell population interaction with *F. hepatica*.

Considering the critical role of  $\gamma\delta$  T cells in cattle immune responses, as well as the specific characteristics of the local immune response in non-fertile CE cysts, our objective is to characterize the presence of these cells in this context. Furthermore, because *Fasciola hepatica* is highly prevalent in cattle and has the capacity to modulate immune responses to other pathogens, we sought to determine whether co-infection affects the  $\gamma\delta$  T cell population of the local immune response in non-fertile CE-cysts.

## Results

### Parasite sample genotypes and morphological features

All parasite samples belonged to *E. granulosus* sensu stricto. Sanger sequencing revealed 3 identical samples that belong to the “founder” haplotype Eg01 (Acc. No. JQ250806), other samples belonged to known haplotypes Eg39 (Acc. No. AB688616), EgCL01 (Acc. No. KX227116), EgCL03 (Acc. No. KX227118) and EgMGL5 (Acc. No. AB893246). No new sequences were generated regarding *E. granulosus* sensu stricto haplotypes. All non-fertile CE cysts samples in this study were unilocular, with white or yellow inner chamber and clear translucent hydatid fluid (Fig. 1A), which are the most common presentation of the metacestode<sup>31</sup>. Histologically, all samples included in the study had the presence of the germinal layer, laminated layer and adventitial layer (Fig. 1B). For examination purposes, we separated the adventitial layer into two areas: the inflammatory infiltrate (Inf), that is located next to the laminated layer, and the surrounding fibrosis (Fib) (Fig. 1B, C).

### Localization and distribution assessment of $\gamma\delta$ T cells

In the adventitial layer of CE cysts, irrespective of FH co-infection,  $\gamma\delta$  T cells are consistently distributed throughout the tissue in all examined samples (Supplementary Fig. 1).  $\gamma\delta$  T cells exhibited a dispersed distribution, with smaller and less frequent clusters. An apparent enrichment of  $\gamma\delta$  T cells was observed in the region of inflammatory infiltration (Inf) between the laminated layer and the fibrosis (Fib), in comparison to the fibrosis itself. Occasional small clusters of  $\gamma\delta$  T cells were found situated between the liver parenchyma and the adventitial layer fibrosis (Fig. 2A) and at the opposite edge towards the inflammatory infiltrate (Fig. 2B). All analyzed CE cysts samples, had a disperse infiltration of  $\gamma\delta$  T cells within the fibrosis (Fig. 2C). In the inflammatory infiltrate area of the adventitial layer, they are found encircling and infiltrating lymphoid cell aggregates (Fig. 2D and E) and integrated within diffuse lymphocytes (Fig. 2F). An image of an adventitial layer lymphoid cell aggregate, can be found in Supplementary Fig. 2.

To quantify  $\gamma\delta$  T cells in the adventitial layer of CE cysts and in tissue controls, double immunofluorescence was employed, targeting CD3 and TCR $\gamma\delta$ , analyzed with confocal imaging (Figs. 3 and 4), numerical data is shown in Table 1. In the inflammatory infiltrate and fibrosis of the adventitial layer in the CE + FH- study group (Fig. 3), the average T cell densities were  $2,323 \pm 727$  CD3+ cells/mm<sup>2</sup> in the AL-Inf area and  $1,088 \pm 428$  CD3+ cells/mm<sup>2</sup> in the AL-Fib area. The mean density of  $\gamma\delta$  T cells in the inflammatory infiltrate and fibrosis was  $620 \pm 298$  and  $315 \pm 215$  TCR $\gamma\delta$  + cells/mm<sup>2</sup>, respectively. In both areas,  $\gamma\delta$  T cells constituted a comparable percentage of the CD3+ cells, amounting to  $26.1 \pm 7.4\%$  in the AL-Inf and  $27.4 \pm 9.3\%$  in the AL-Fib. The inflammatory infiltrate in the AL exhibited a significant 2.1-fold increase in the total T cell count compared to the AL fibrosis. Interestingly,  $\gamma\delta$  T cell count and the proportion of TCR $\gamma\delta$  + cells within the CD3+ population, was not statistically significant.

In the adventitial layer of the CE + FH + group (Fig. 3), the inflammatory infiltrate and fibrosis exhibited average T cell densities of  $2,154 \pm 631$  CD3+ cells/mm<sup>2</sup> and  $646 \pm 284$  CD3+ cells/mm<sup>2</sup>, respectively. The mean density of  $\gamma\delta$  T cells in these regions was  $314 \pm 95$  TCR $\gamma\delta$  + cells/mm<sup>2</sup> in the inflammatory infiltrate and  $135 \pm$

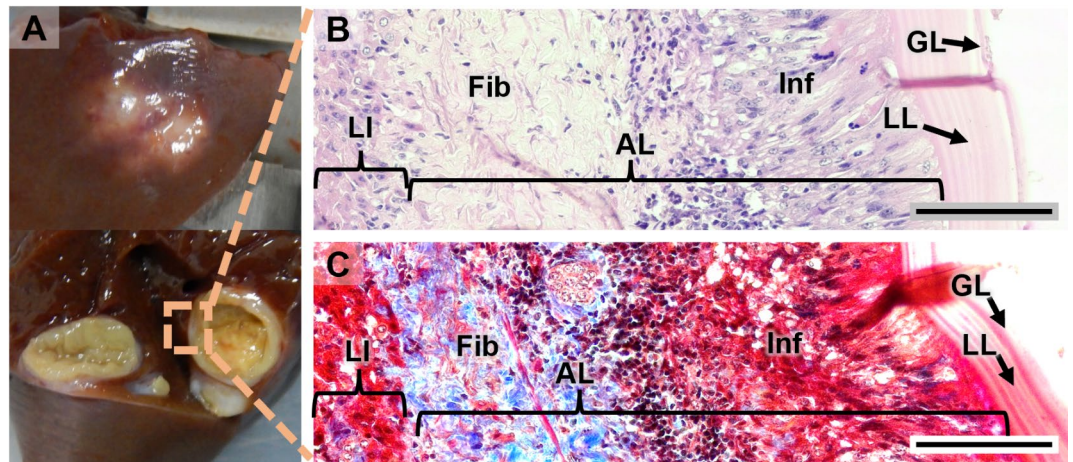


**Fig. 1.** Gross and histological features of *Echinococcus granulosus sensu stricto* cattle liver CE cysts. (A) Gross pictures of an *Echinococcus granulosus sensu stricto* liver metacestode, intact (up) and opened (down). (B) Bright-field image of 5 µm-thick paraffin-embedded sections of the adventitial layer (AL) of non-fertile CE-cysts with hematoxylin eosin staining. (C) Bright-field image of 5 µm-thick paraffin-embedded sections of the adventitial layer (AL) of non-fertile CE-cysts with Masson trichrome staining. LI: surrounding liver tissue; Fib: Adventitial layer fibrosis; Inf: Adventitial layer inflammatory infiltrate; GL: Germinal Layer; LL: Laminated Layer. Scale bar = 100 µm.

113 TCR $\gamma\delta$  + cells/mm<sup>2</sup> in the fibrosis. In both areas,  $\gamma\delta$  T cells represented a similar proportion of the CD3+ cell population, accounting for 15.4 ± 5.8% in the AL-Inf and 18.7 ± 7% in the AL-Fib. In the adventitial layer of CE + FH + cases, the inflammatory infiltrate showed a significant 3.3-fold increase in total T cell count compared to the AL fibrosis. Like the CE + FH- group, the difference in  $\gamma\delta$  T cell counts or  $\gamma\delta$  T/total T cell proportion between the two areas was not statistically significant.

In CTRL and FH + liver tissue controls, the presence of  $\gamma\delta$  T cells was scarce and uniformly distributed throughout the parenchyma (Par), irrespective of FH infection. A notably higher density of these cells was observed in the portal areas (PA), particularly in FH + cases (Supplementary Fig. 2).

In the parenchyma and portal areas (Fig. 4) of CTRL livers, the average T cell density was 340 ± 188 ( $n$  = 5) and 800 ± 258 ( $n$  = 5) CD3+ cells/mm<sup>2</sup>, respectively. The mean density of  $\gamma\delta$  T cells in these areas was 12 ± 8 TCR $\gamma\delta$  + cells/mm<sup>2</sup> (CTRL LI-Par) and 51 ± 18 TCR $\gamma\delta$  + cells/mm<sup>2</sup> (CTRL LI-PA).  $\gamma\delta$  T cells accounted for 3.7 ± 2.7% of CE + cells in the parenchyma and 6.6 ± 2.1% of CD3+ cells in the portal areas. As anticipated, portal areas exhibited a significantly higher number of both  $\gamma\delta$  T cells and the total T cell population compared to the parenchyma, showing an increase of 2.3 and 4.25-fold, respectively. However, the proportion of TCR $\gamma\delta$  + cells within the CD3+ population was found to be similar in both areas.

In the parenchyma and portal areas of FH + livers (Fig. 4), the mean T cell densities were 187 ± 72 ( $n$  = 5) and 663 ± 345 ( $n$  = 5) CD3+ cells/mm<sup>2</sup>, respectively. The mean densities of  $\gamma\delta$  T cells in these areas were 11 ± 7 TCR $\gamma\delta$  + cells/mm<sup>2</sup> for FH + LI-Par and 79 ± 67 TCR $\gamma\delta$  + cells/mm<sup>2</sup> for FH + LI-PA. Consistent with expectations, portal areas had a significantly higher total T cell population compared to the parenchyma, with a 7.3-fold increase. Although the mean count of  $\gamma\delta$  T cells was 3.5-fold higher in portal areas compared to the parenchyma, this was not found to be statistically significant ( $p$  = 0.0513). Interestingly, the proportion of TCR $\gamma\delta$  + cells within the CD3+ population was 1.9 times higher in portal areas at 11.4%, compared to 6% in the parenchyma.

In our analysis of  $\gamma\delta$  T cells as a proportion of the total T cell population, no significant differences were noted between the different analyzed areas across most groups. Therefore, we calculated the overall proportion of  $\gamma\delta$  T cells within the total T cell population, regardless of area. We observed that tissue controls had the lowest proportions, with  $\gamma\delta$  T cells comprising 5 ± 1.1% in CTRL and 10 ± 3.4% in FH + groups; no significant differences were found between these two groups. The CE + FH- group exhibited the highest proportion, with  $\gamma\delta$  T cells constituting 26.8 ± 6.8% of total T cells, significantly higher than the tissue controls (4.8/2.6-fold higher than CTRL/FH). In cases of CE with FH co-infection (CE + FH+), the proportion of  $\gamma\delta$  T/total T cells was 1.6-fold lower than in CE + FH-, a statistically significant difference. Interestingly, CE + FH + group had no significant differences compared to the FH + control. Nevertheless, the proportion of  $\gamma\delta$  T cells in the CE + FH + group (16.5 ± 6.3%) was significantly higher than in the CTRL group by 2.9-fold (Fig. 5).

## Discussion

It has been repeatedly suggested that the local immune response to CE cysts is associated with parasite viability<sup>7-9</sup>. In recent years, advancements have been made in characterizing the local immune response in different intermediate hosts, where CD3+ lymphocytes have been consistently identified as a major component of the local immune response<sup>32-35</sup>. We previously described that the amount of T cells (CD3+) in the adventitial layer was associated with fertility in cattle CE cysts<sup>14</sup>.

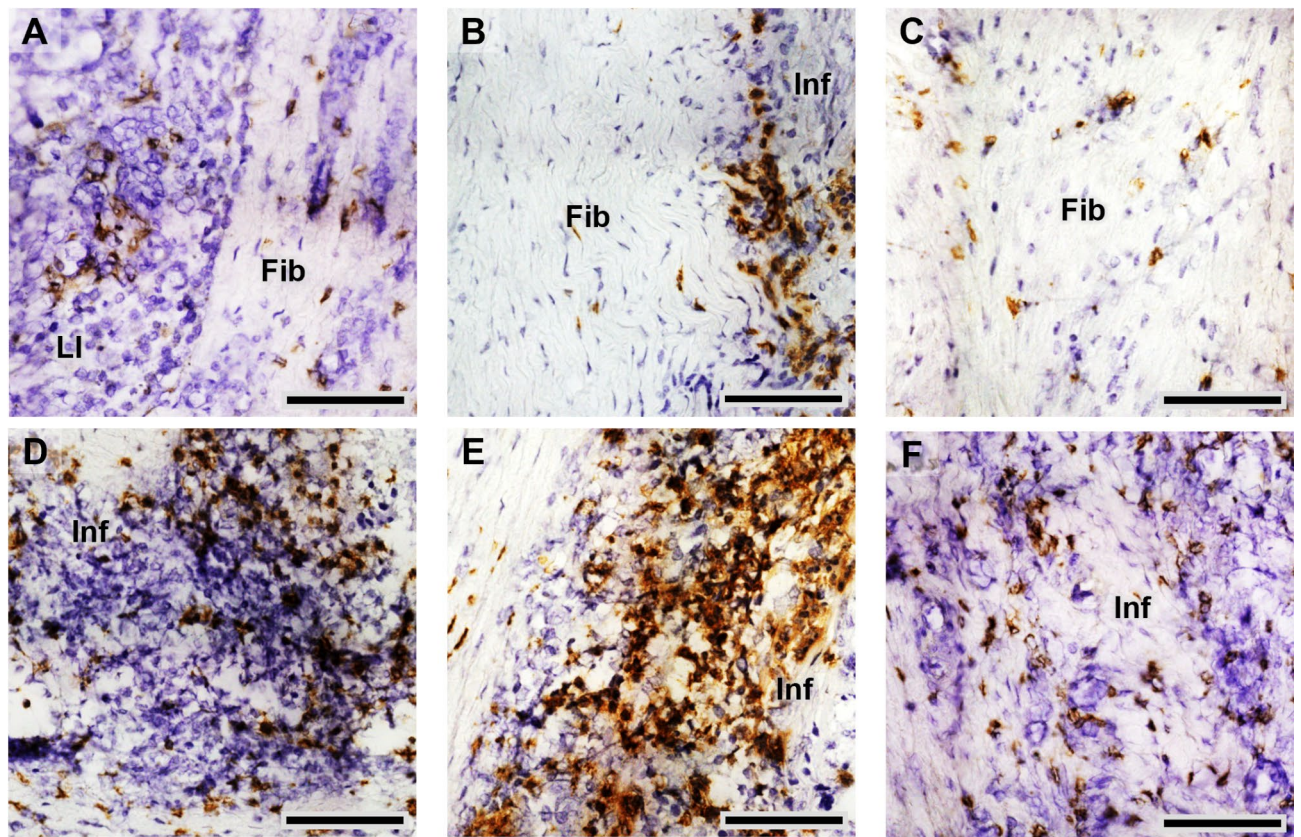


**Fig. 2.**  $\gamma\delta$  T distribution pattern in the adventitial layer of non-fertile CE cysts. Bright-field images of immunohistochemical detection of TCR $\gamma\delta$  in 10  $\mu$ m-thick frozen liver sections of the adventitial layer (AL) of non-fertile CE-cysts. (A)  $\gamma\delta$  T cells infiltrating AL fibrosis and surrounding liver tissue. (B)  $\gamma\delta$  T cells surrounding and within the AL fibrosis. (C) Disperse infiltration within AL fibrosis. (D)  $\gamma\delta$  T cells encircling lymphoid cell aggregates in the inflammatory infiltrate of the AL. (E)  $\gamma\delta$  T cells in clusters infiltrating lymphoid cell aggregates. (F)  $\gamma\delta$  T cells constituting part of diffuse lymphocytes of the inflammatory infiltrate in the AL. TCR $\gamma\delta$  +  $\gamma\delta$  T cells are shown in brown, counterstained with hematoxylin. LI: surrounding liver tissue; Fib: Adventitial layer fibrosis; Inf: Adventitial layer inflammatory infiltrate; AL: Adventitial layer; LL: Laminated layer Scale bar = 100  $\mu$ m.

Various approaches have been used to characterize the population of CD3<sup>+</sup> cells in the local immune response to CE cysts, involving the expression of CD4 or CD8<sup>32,34</sup>, but none have included the role of  $\gamma\delta$  T cells. In cattle,  $\gamma\delta$  T cells are an important subset of T lymphocytes involved in the immune response to various diseases affecting this species<sup>36</sup>. To the best of our knowledge, this is the first description of the  $\gamma\delta$  T cell local immune response in non-fertile CE cysts in cattle.

In this study, through immunohistochemistry, we found that CD3<sup>+</sup> lymphocytes are aggregated in the adventitial layer of non-fertile CE cysts, consistent with descriptions in humans<sup>32</sup>. Through immunofluorescence, we found that they are present in higher numbers than in non-infected liver controls, as has been observed in sheep with non-fertile CE cysts<sup>35</sup>.

In cattle, the adventitial layer of non-fertile CE cysts is a granulomatous reaction<sup>8</sup>, composed of inflammatory infiltrate surrounded by a fibrous capsule<sup>37</sup>. In this work, we found that CD3<sup>+</sup> lymphocytes are in higher numbers in the inflammatory infiltrate than within the fibrous layer, showing a differential distribution within the adventitial layer in this species. In non-infected liver tissue controls, CD3<sup>+</sup> cells also had a differential distribution, with higher numbers in portal areas compared to those infiltrating the liver parenchyma, as previously described in humans<sup>38</sup>.

Our previous work showed that co-infection with *Fasciola hepatica*, a common trematode in cattle, was associated with changes in anatomopathological characteristics and immune response components in cattle with CE<sup>25,31,39,40</sup>. In this study, we analyzed co-infection with FH as a variable to see if associations were found in the characterization of  $\gamma\delta$  T cells in the adventitial layer of non-fertile CE cysts.

Immunohistochemistry (IHC) results show that, regardless of FH co-infection,  $\gamma\delta$  T cells are present throughout the adventitial layer, within the inflammatory infiltrate and surrounding fibrosis. Unlike total T cells,  $\gamma\delta$  T cells exhibited a more dispersed distribution in the adventitial layer, with smaller and less frequent clusters. Through double immunofluorescence, we quantified in situ  $\gamma\delta$  T cells and estimated the proportion of  $\gamma\delta$  T cells from total T cells (CD3<sup>+</sup>).  $\gamma\delta$  T cell counts showed no statistically significant difference between the inflammatory infiltrate and the fibrosis of non-fertile CE cysts in both animals with FH + and those without co-

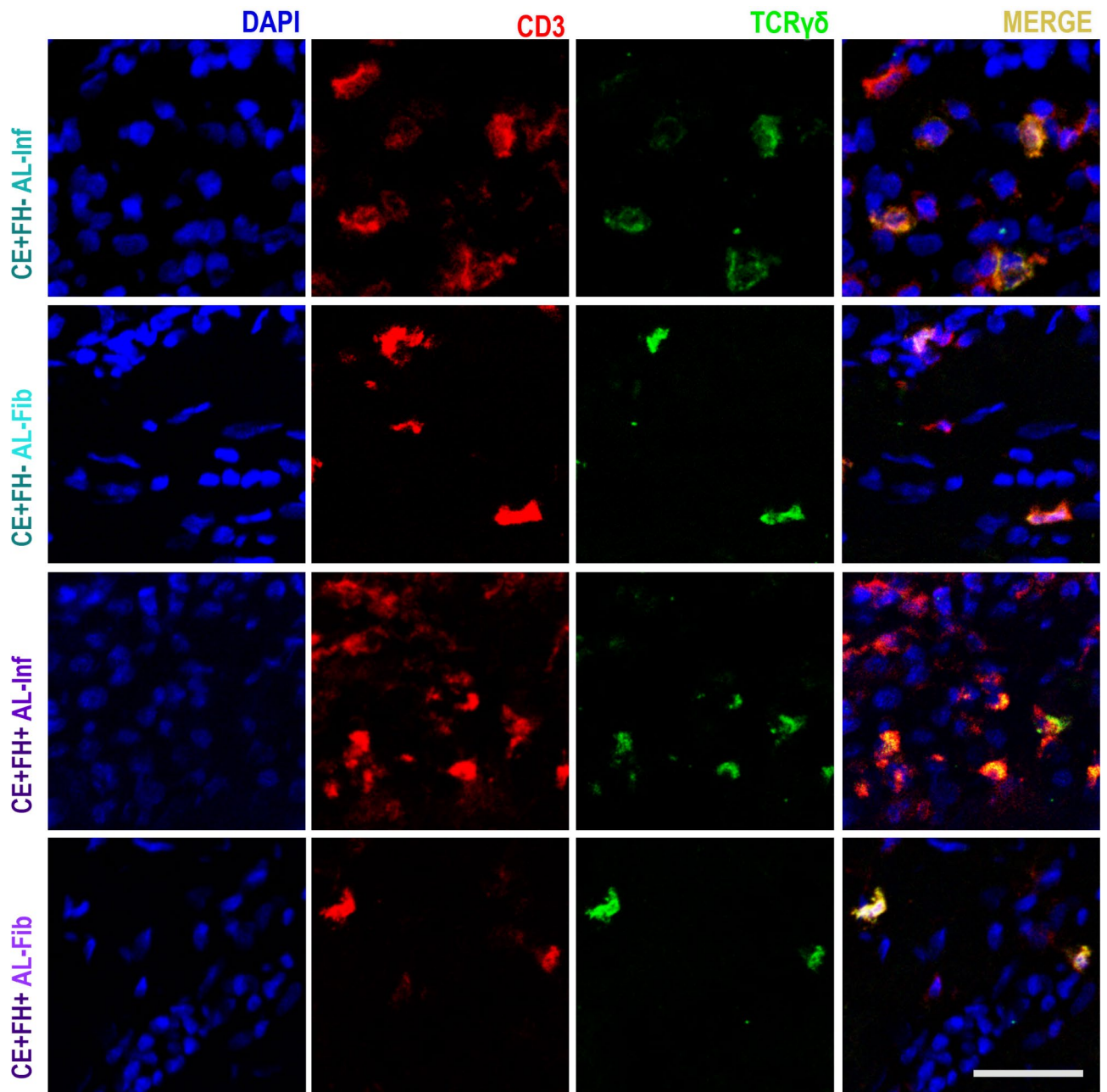


**Fig. 3.**  $\gamma\delta$  T and Total T cells in fibrotic and inflammatory areas of the adventitial layer in non-fertile CE-Cysts, with or without *Fasciola hepatica* co-infection. Confocal immunofluorescence images of 10  $\mu\text{m}$ -thick frozen liver tissue sections of the Inflammatory infiltrate (AL-Inf) and fibrosis (AL-Fib) in AL of a representative non-fertile CE cyst with and without *Fasciola hepatica* co-infection. CD3+ total T cells are marked in red, TCR $\gamma\delta$  + cells in green, CD3+ TCR $\gamma\delta$  +  $\gamma\delta$  T cells in yellow/orange. Scale bar = 20  $\mu\text{m}$ .

infection. However, when clustered together as just CE+,  $\gamma\delta$  T cell counts showed a statistical difference between the two areas. It is plausible that this discordance in the results is due to the smaller number of samples in the analysis when co-infection was included as a variable.

To compare our  $\gamma\delta$  T cell distribution results, we looked at commonly studied granulomatous diseases in ruminants, such as mycobacterial disease models, where  $\gamma\delta$  T cells seem to play an important role<sup>41</sup>. However, in this subject, most publications describe the  $\gamma\delta$  T population by the expression of workshop cluster 1 (WC1 in cattle, T19 in small ruminants), which is only expressed in a subtype of  $\gamma\delta$  T cells, and not the global  $\gamma\delta$  T population as assessed by TCR  $\gamma\delta$  presence like in this work. One study described, in a *Mycobacterium avium* subspecies *paratuberculosis* (*Map*) disease model, the presence of TCR  $\gamma\delta$  + cells in different stages and their association with granuloma organization. They found that  $\gamma\delta$  T cells are recruited to the granuloma from the initial stages of the lesion and are present in the late stages in highly organized granulomas. However, no description of the distribution of  $\gamma\delta$  T cells or comparable numerical data was provided. It is noteworthy that non-fertile

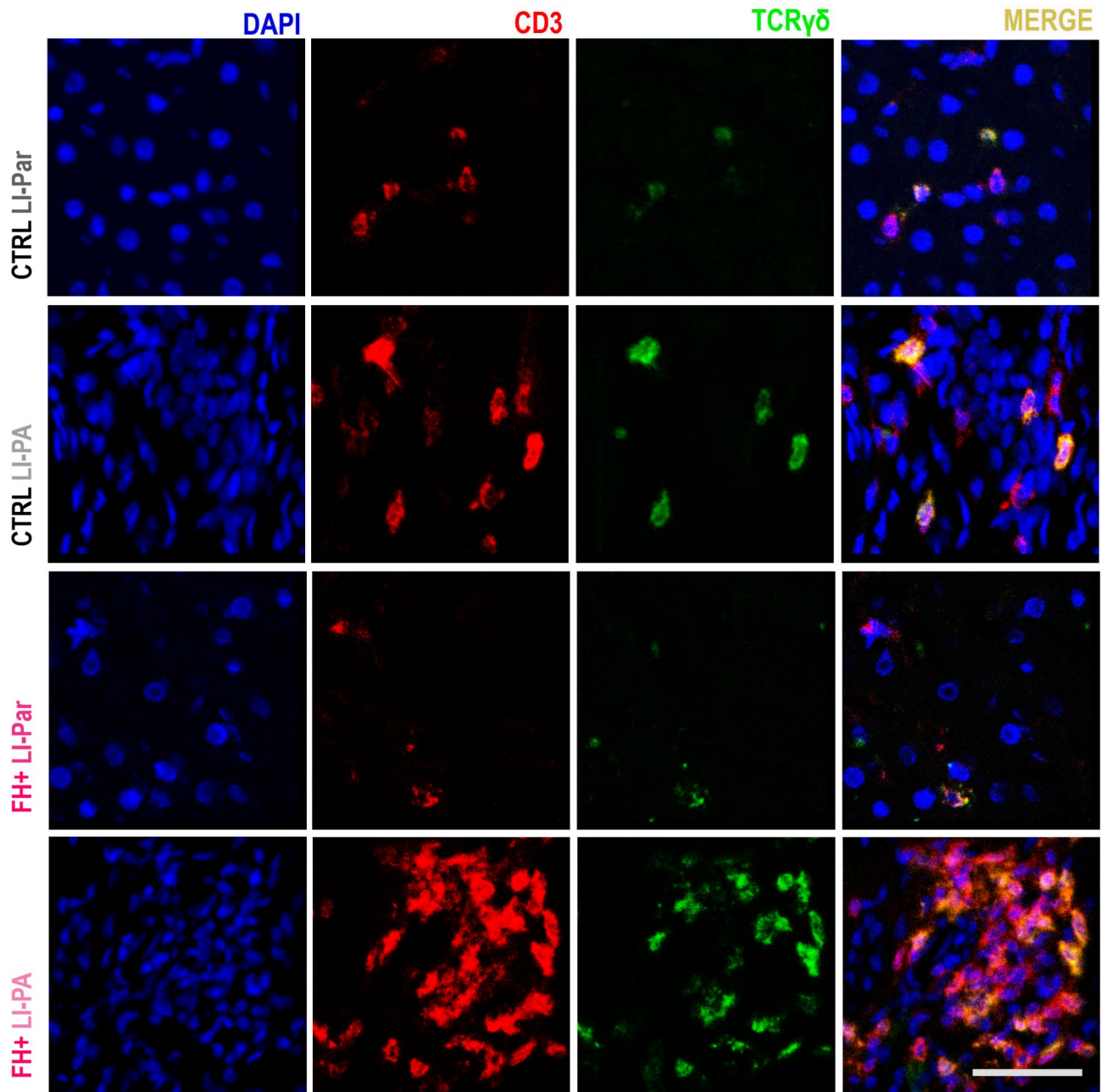


**Fig. 4.**  $\gamma\delta$  T and Total T Cells in the parenchyma and portal areas of clinically non-infected liver tissues and *Fasciola hepatica* infected liver tissues. Confocal immunofluorescence images of 10  $\mu\text{m}$ -thick frozen liver tissue sections of CTRL or FH + animals, focusing on the liver parenchyma (Par) or portal areas (PA); CD3+ total T cells marked in red, TCR $\gamma\delta$  + cells in green, CD3+ TCR $\gamma\delta$  +  $\gamma\delta$  T cells in yellow/orange. Scale bar = 20  $\mu\text{m}$ .

bovine CE cysts are histologically similar to what is described for the late stages of this type of granuloma<sup>42</sup>. In an experimental infection of *Mycobacterium bovis*,  $\gamma\delta$  T cells were estimated in a semiquantitative manner through a score of immunohistochemistry, representing a small count in the granuloma that decreased with the consolidation of the granuloma<sup>43</sup>.

As demonstrated in this work, the percentage of  $\gamma\delta$  T cells among CD3+ cells were similar across the studied areas in non-fertile CE cysts. For comparative analysis, the percentage of  $\gamma\delta$  T cells was estimated using consolidated data from both areas. We found that the  $\gamma\delta$  T cell population, in proportion to total T cells, is enriched in the adventitial layer of non-fertile CE cysts, both with and without FH co-infection, compared to non-infected controls. This suggests that  $\gamma\delta$  T cells are recruited to CE cysts similarly to the aforementioned granulomatous diseases.

Interestingly, in most FH + liver samples, we observed denser immunolabeling of  $\gamma\delta$  T cells in portal areas compared to the parenchyma and tissue controls. Although no statistically significant increase was found in raw  $\gamma\delta$  T cell counts, there was an enrichment in the proportion of  $\gamma\delta$  T cells among CD3+ cells in portal areas, and

Study group	n	Area	CD3+ cells/mm <sup>2</sup> count		TCRγδ + cells/mm <sup>2</sup> count		TCRγδ+/CD3+ percentage (%)	
			Mean ± SD	P-value	Mean ± SD	P-value	Mean ± SD	P-value
CE + FH-	4	AL-Inf	2,323 ± 727	0.0264*	620 ± 298	0.1478	26.1 ± 7.4	0.8278
		AL-Fib	1,088 ± 428		315 ± 21		27.4 ± 9.3	
CE + FH+	4	AL-Inf	2,154 ± 631	0.0048*	314 ± 95	0.052	15.4 ± 5.8%	0.5047
		AL-Fib	646 ± 284		135 ± 113		18.7 ± 7%	
CTRL	5	AL-Inf	340 ± 188	0.0168*	12 ± 8	0.0019*	3.7 ± 2.7%	0.1032
		AL-Fib	800 ± 258		51 ± 18		6.6 ± 2.1%	
FH+	5	AL-Inf	187 ± 72	0.0165	11 ± 7	0.0513	6 ± 3.2	0.0479*
		AL-Fib	663 ± 345		79 ± 67		11.4 ± 4.1	

**Table 1.** CD3+ and TCRγδ + cell counts in CE cysts and tissue controls with/without *Fasciola hepatica* co-infection. Data represents mean ± Standard deviation (SD) of cell counts per mm<sup>2</sup> or percentage of TCRγδ + in CD3+ population. Percentages and counts derived from the count of positive cells from 6 ROIs per sample, each with an area of 37,539 μm<sup>2</sup>. Statistical significance assessed with student t-test (p-value < 0.05); \*p < 0.05. CE+. CE + FH-: non-fertile CE cysts non-co-infected with *Fasciola hepatica*; CE + FH+: non-fertile CE cysts co-infected with *Fasciola hepatica*, AL: Adventitial Layer, Inf: Inflammatory infiltrate, Fib: fibrosis, CTRL: control tissue for non-infected animal, FH+: *Fasciola hepatica* tissue control, LI: Liver, Par: Parenchyma, PA: Portal area.

an increase in γδ T cell counts in portal areas compared to the same region in non-infected controls. Consistent with these results, one study showed that in vitro PBMC proliferate in response to *F. hepatica* antigens<sup>29</sup>. Given that *F. hepatica* adult parasites reside in bile ducts, it is expected that portal areas, which contain small bile ducts, are exposed to FH antigens. The increase in γδ T cell proportion in the portal areas of FH + samples did not affect the overall proportions of γδ T cells in the tissue, as comparison to non-infected controls showed no significant difference.

In situ analyses have been performed in small ruminants like sheep and goats. However, due to their smaller size, hepatic lesions caused by *F. hepatica* and the clinical outcomes tend to be more severe in these species compared to cattle, where the infection is commonly asymptomatic<sup>44,45</sup>. A study in goats infected with FH found that γδ T cells were occasionally seen in the inflammatory infiltrate associated with chronic hepatic lesions and in the gallbladder<sup>46</sup>. Another study in sheep found that in primary chronic fascioliasis, γδ T cells were a prominent feature in the fibrotic strands of peribulbar liver fibrosis<sup>47</sup>, which supports our finding of γδ T cells in the fibrous layer of non-fertile CE cysts.

It has been suggested that γδ T cells downregulate alpha beta (αβ) T cell proliferation in response to *F. hepatica* antigens<sup>29</sup>, and that inhibition of αβ T cells would not be beneficial for parasite survival, as αβ T cells respond in a non-effective Th2/Treg manner<sup>48</sup>. In the present work, although no correlation analysis was made between the γδ T cell proportion and total CD3 counts, the presence of FH in liver tissues with or without CE did not change CD3+ cell counts. Further in vivo work is needed to determine whether fluke burdens of *F. hepatica* infection or the degree of organ damage affects the dynamics within the global T cell population and γδ T cell proportion in the parenchyma and portal areas.

Although in this study total T cell count were not affected by coinfection as we had previously reported<sup>14</sup>, we found that co-infected animals had fewer γδ T cells in proportion to CD3+ cells compared to those without co-infection, and when comparing co-infected animals with FH only (FH+), no difference was found. This would suggest an immunoregulatory effect of FH co-infection in the γδ T cell population. This is consistent with previous results, where we compared adventitial layer features associated with granulomatous response and found that co-infection was associated with an absence of both lymphoid follicles and palisading macrophages in the adventitial layer of liver CE cysts<sup>31</sup>. It is plausible, that as in other granulomatous diseases in cattle, γδ T cells could be involved in the organization of the granuloma in non-fertile CE cysts, however further studies are needed to establish an association between these features and γδ T proportion.

## Materials and methods

### Sample collection

Parasite samples were obtained at abattoirs; during routine cattle slaughtering, individual identification of animals was conducted. Visceral organs, mainly the lungs and liver, were inspected by visual examination, palpation, and incisions by the abattoirs' official veterinary inspectors, for the presence of CE cysts and FH, as previously described<sup>25</sup>. Liver tissue samples and suspected CE cysts were removed, placed in separate hermetically sealed polythene bags, and transported in an isothermal container within 3 h to be further processed in the laboratory. All sampling protocols were approved by the Bioethics Committee of Universidad Andres Bello (resolution N° 034/2020).

### Sample processing

For CE cyst confirmation and processing, cystic structures were first aspirated with a sterile 10 ml syringe with a 21 g hypodermic needle to reduce intracystic fluid pressure and to visually examine the fluid (color, texture,

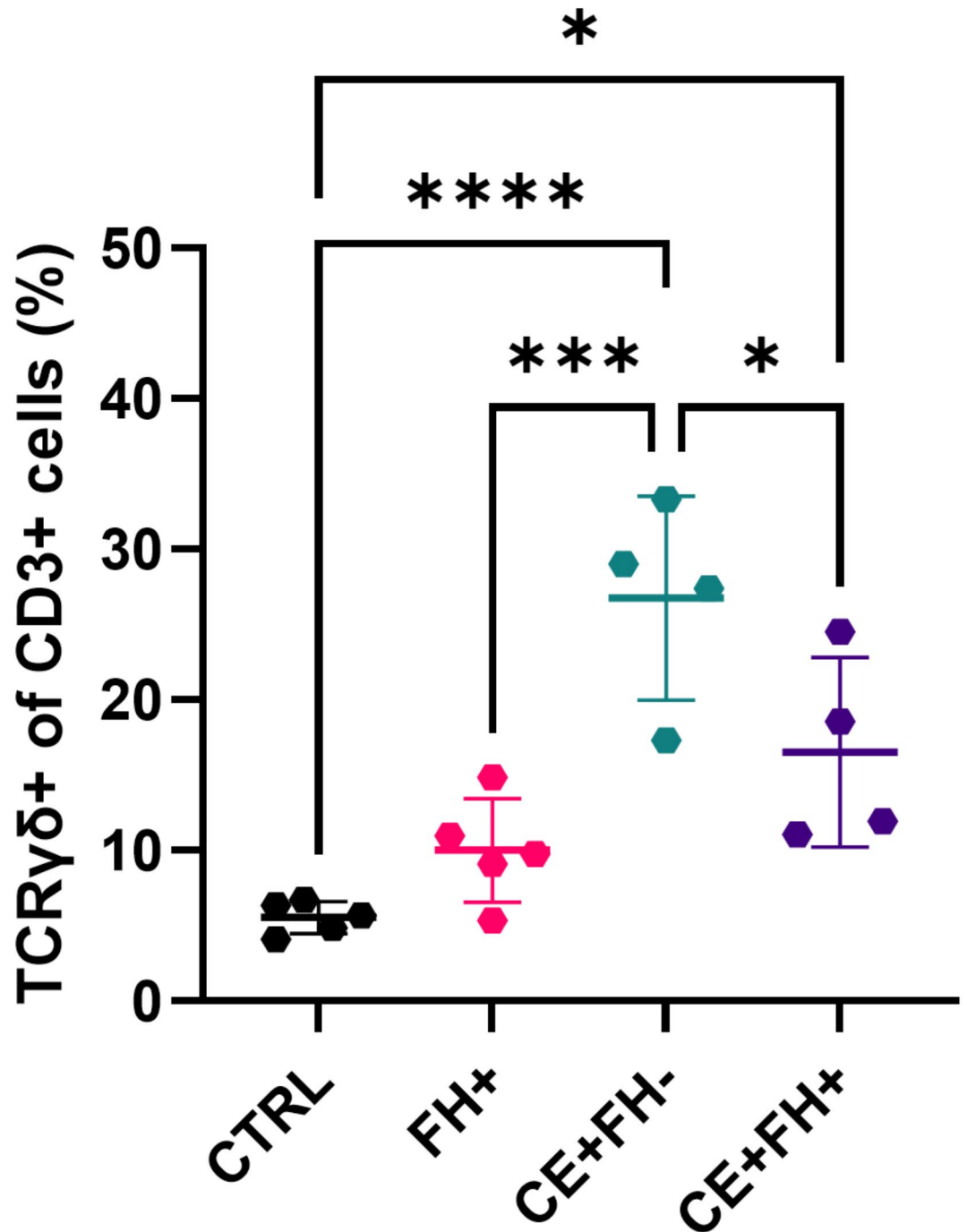


**Fig. 5.** Proportion comparison of  $\gamma\delta$  T cells in CE cysts and tissue controls with/without *Fasciola hepatica* co-infection.  $\gamma\delta$  T cells (CD3+, TCR $\gamma\delta$ +) proportion within total T cells (CD3+) of non-infected tissue controls (CTRL), *Fasciola hepatica* tissue control (FH+), adventitial layer of non-fertile CE cysts non-co-infected with *Fasciola hepatica* (CE + FH-) and co-infected (CE + FH+). Data represents mean  $\pm$  SD of cell counts per mm<sup>2</sup>. Percentages and counts derived from the count of positive cells from 12 ROIs per sample, each with an area of 37,539  $\mu\text{m}^2$ . Analysis via confocal double-targeted immunofluorescence (CD3 and TCR $\gamma\delta$ ) in 10  $\mu\text{m}$ -thick sections. Statistical significance assessed with ANOVA with Bonferroni multiple comparison analysis (p-value < 0.05); \* $p$  < 0.05, \*\*\* $p$  < 0.001, \*\*\*\* $p$  < 0.0001.

and viscosity). The cysts were then opened along their longest longitudinal axis using a sterile disposable scalpel blade, and fertility was assessed as previously described<sup>8</sup>. The inner wall (germinal layer) of one half of the cyst was carefully swabbed using the tip of a microbiological transport swab embedded with hydatid fluid, and the swab tip was placed in a 1.5 ml tube for DNA extraction. A section of the other half of the cyst was placed in aluminum molds, covered in OCT compound, and frozen by direct immersion in liquid nitrogen-chilled solid

isopentane. The remaining tissue was used to perform routine Haematoxylin-eosin stainings, as well as Masson Trichrome histochemistry assay.

### Parasite genotyping

Double-stranded DNA (dsDNA) from the germinal layer was extracted using the Relia-Prep gDNA Tissue Miniprep System (Promega). The full mitochondrial *cox1* gene (1609 bp) was amplified via PCR, following a previously described protocol<sup>10</sup>. Positive samples were subsequently purified, and Sanger sequenced at an external service. Sequencing analysis was conducted using Geneious Prime<sup>®</sup> v2025.0.3, with the *Echinococcus granulosus* sensu stricto genotype determined using the *E. granulosus* s.s. haplotype “Eg01” as the reference sequence (Accession No. JQ250806), manually checking peak data when discrepancies arose. Only samples that belonged to the *E. granulosus* s.s. genotype were included in this study.

### Study groups and selection criteria

Animals identified as CE + in this study had one or more non-fertile CE cysts. Non-fertile CE cyst samples were selected based on both macroscopic and microscopic criteria, conforming to the classic non-fertile bovine CE cyst characteristics as previously described<sup>31</sup>.

Study groups were defined as follows: Non-fertile CE cysts of cattle without *Fasciola hepatica* co-infection (CE + FH-) and with *F. hepatica* co-infection (CE + FH+). Liver sections from cattle without CE (CTRL) and with *F. hepatica* infection (FH+) were used as controls. Control animals were selected based on passing both antemortem and postmortem inspections. Antemortem inspection ensured animals were free of visible alterations, and postmortem inspection confirmed the absence of macroscopically identifiable diseases or associated tissue parasitosis in their carcasses, except for *F. hepatica* in the FH + controls.

A total of 18 samples passed all the mentioned criteria and were included in the study: 4 CE + FH-, 4 CE + FH+, 5 CTRL, and 5 FH+.

### Immunohistochemistry and double Immunofluorescence

For in situ  $\gamma\delta$  T cell characterization, single immunohistochemistry (IHC), and double indirect immunofluorescence (IF) targeting both CD3 and  $\gamma\delta$  TCR were performed on frozen tissues. Frozen tissue samples were sectioned at a thickness of 10  $\mu\text{m}$  in a cryostat and mounted individually on positively charged slides. All samples were checked for structural tissue integrity using hematoxylin-eosin dye.

For IHC and IF, frozen sections were washed with PBS (Phosphate Buffered Saline, pH 7.4) for 5 min. For slides destined for IF, an autofluorescence blocking step was added: slides were incubated for 30 min in 0.5% Sudan black solution in 70% ethanol at RT, protected from light in a humidity chamber, and then washed for 10 min with deionized water<sup>49</sup>. All slides had nonspecific binding sites blocked with Pro-Block (ScyTek) for 30 min in a humidity chamber at RT. Samples for IHC or IF were incubated overnight at 4 °C with Pro-Block diluted primary antibodies: Rabbit IgG anti-Human CD3 (1:500 for IHC and 1:400 for IF) (Dako ref. A0452) and/or Mouse IgG2b anti-Bovine  $\gamma\delta$  TCR (1:250 for IHC 1:200 for IF) (Clone GB21A, Kingfisher Biotech, ref. WSC0578B-100) or only Pro-Block for technical negative controls.

After primary antibody incubation, all slides were washed three times with 0.05% Tween 20<sup>®</sup> in PBS (PBS-T). For IHC procedures, endogenous peroxidase blocking was performed with 3% hydrogen peroxide for 30 min and washed with PBS-T.

For antibody detection, all slides (including negative controls) were incubated for 2 h at RT, protected from light in a humidity chamber, with matching secondary antibodies (From Jackson ImmunoResearch) at a 1:200 dilution in Pro-Block. For IHC, Horseradish Peroxidase conjugated Goat anti-Mouse IgG (H + L) (115-035-062) or Goat anti-Rabbit IgG (H + L) (111-035-144) was used. For IF a combination of Alexa Fluor<sup>®</sup> 647 conjugated Goat anti-Rabbit IgG (H + L) (111-605-003) and Alexa Fluor<sup>®</sup> 488 Alpaca anti-Mouse IgG (H + L) (615-545-214) were used. After incubation, samples were washed four times with PBS-T. Slides for IF were mounted with Fluoromount-G<sup>™</sup> (Invitrogen), while slides for IHC were treated with the DAB substrate kit (Vector Laboratories), counterstained with hematoxylin, dehydrated, and mounted with Neo-Mount<sup>™</sup>.

Fluorescently detected samples were examined using a Leica TCS SP8 confocal microscope (Leica Microsystems) and processed with Leica Application Suite X (Leica Microsystems). Positive cells were estimated manually in 37,539  $\mu\text{m}^2$  images by a third-party technician. Using Image J 1.44p software (National Institutes of Health, USA), a projection in each color channel was made from 5 images covering a total depth of 4  $\mu\text{m}$ , by selecting average intensity using z-project tools, to then merge the channels. Positive cells were manually marked by mouse clicks on merged images and then recorded by the Cell Counter tool in Analyze plugins. Cell proportions were estimated by dividing  $\gamma\delta$  TCR + cells within the CD3+ population as described previously<sup>50</sup>. Brightfield observable samples were examined and scanned using a Leica DM300 microscope with a Microvisioner manual whole slide imaging system. Selected regions of interest were also photographed with an Olympus FSX100 inverted microscope.

### Statistical analysis

Data was analyzed using GraphPad Prism version 8.00. Data distribution was assessed by the Shapiro–Wilk test. T-tests and ANOVA, followed by post hoc analysis with Tukey or Bonferroni tests, were used as appropriate. P values below 0.05 were considered statistically significant.

### Data availability

The datasets generated and analyzed during the current study are available in GenBank repository, Accession Numbers JQ250806, AB688616, KX227116, KX227118, and AB893246. No new sequences were generated regarding *E. granulosus* sensu stricto haplotypes.

Received: 13 December 2024; Accepted: 24 March 2025

Published online: 28 March 2025

## References

- Agudelo Higueta, N. I., Brunetti, E. & McCloskey, C. Cystic echinococcosis *J. Clin. Microbiol.* **54**, 518–523. (2016).
- Alvarez Rojas, C. A. et al. High intraspecific variability of *Echinococcus granulosus sensu stricto* in Chile. *Parasitol. Int.* **66**, 112–115 (2017).
- Alvarez Rojas, C. A., Romig, T. & Lightowers, M. W. *Echinococcus granulosus sensu lato* genotypes infecting humans—review of current knowledge. *Int. J. Parasitol.* **44**, 9–18 (2014).
- Vuitton, D. A. et al. International consensus on terminology to be used in the field of echinococcoses. *Parasite* **27**, 41 (2020).
- Thompson, R. C. Biology and systematics of *Echinococcus*. *Adv. Parasitol.* **95**, 65–109 (2017).
- Rogan, M. T., Bodell, A. J. & Craig, P. S. Post-encystment/established immunity in cystic echinococcosis: is it really that simple? *Parasite Immunol.* **37**, 1–9 (2015).
- Diaz, A. Immunology of cystic echinococcosis (hydatid disease). *Br. Med. Bull.* **124**, 121–133 (2017).
- Hidalgo, C. et al. New insights of the local immune response against both fertile and infertile hydatid cysts. *PLoS One* **14**, e0211542 (2019).
- Barnes, T. S. et al. Comparative pathology of pulmonary hydatid cysts in macropods and sheep. *J. Comp. Pathol.* **144**, 113–122 (2011).
- Hidalgo, C., Stoores, C., Pereira, I., Paredes, R. & Alvarez Rojas, C. A. Multiple haplotypes of *Echinococcus granulosus sensu stricto* in single naturally infected intermediate hosts. *Parasitol. Res.* **119**, 763–770 (2020).
- Siracusano, A. et al. Immunomodulatory mechanisms during *Echinococcus granulosus* infection. *Exp. Parasitol.* **119**, 483–489 (2008).
- Vatankhah, A. et al. Characterization of the inflammatory cell infiltrate and expression of costimulatory molecules in chronic *Echinococcus granulosus* infection of the human liver. *BMC Infect. Dis.* **15**, 530 (2015).
- Vismarra, A. et al. Immuno-histochemical study of ovine cystic echinococcosis (*Echinococcus granulosus*) shows predominant T cell infiltration in established cysts. *Vet. Parasitol.* **209**, 285–288 (2015).
- Jimenez, M. et al. Lymphocyte populations in the adventitial layer of hydatid cysts in cattle: Relationship with cyst fertility status and fasciola hepatica co-infection. *Vet. Pathol.* **57**, 108–114 (2020).
- Sakamoto, T. & Cabrera, P. A. Immunohistochemical observations on cellular response in unilocular hydatid lesions and lymph nodes of cattle. *Acta Trop.* **85**, 271–279 (2003).
- Morath, A. & Schamel, W. W. Alphabeta and gammadelta T cell receptors: Similar but different. *J. Leukoc. Biol.* **107**, 1045–1055 (2020).
- Guzman, E., Price, S., Poulosom, H. & Hope, J. Bovine gammadelta T cells: Cells with multiple functions and important roles in immunity. *Vet. Immunol. Immunopathol.* **148**, 161–167 (2012).
- Telfer, J. C. & Baldwin, C. L. Bovine gamma delta T cells and the function of gamma delta T cell specific WC1 co-receptors. *Cell. Immunol.* **296**, 76–86 (2015).
- Guerra-Maupome, M., Slate, J. R. & McGill, J. L. Gamma delta T cell function in ruminants. *Vet. Clin. Food Anim. Pract.* **35**, 453–469 (2019).
- Pedersen, A. B. & Fenton, A. Emphasizing the ecology in parasite community ecology. *Trends Ecol. Evol.* **22**, 133–139 (2007).
- Cwiklinski, K., O'Neill, S. M., Donnelly, S. & Dalton, J. P. A prospective view of animal and human fasciolosis. *Parasite Immunol.* **38**, 558–568 (2016).
- Elias, D., Britton, S., Kassu, A. & Akuffo, H. Chronic helminth infections may negatively influence immunity against tuberculosis and other diseases of public health importance. *Expert Rev. Anti Infect. Ther.* **5**, 475–484 (2007).
- Salgame, P., Yap, G. S. & Gause, W. C. Effect of helminth-induced immunity on infections with microbial pathogens. *Nat. Immunol.* **14**, 1118–1126 (2013).
- Naranjo Lucena, A., Garza Cuartero, L., Mulcahy, G. & Zintl, A. The immunoregulatory effects of co-infection with fasciola hepatica: From bovine tuberculosis to Johne's disease. *Vet. J.* **222**, 9–16 (2017).
- Stoores, C. et al. *Echinococcus granulosus* hydatid cyst location is modified by fasciola hepatica infection in cattle. *Parasites Vectors* **11**, 542 (2018).
- Graham-Brown, J. et al. Dairy heifers naturally exposed to fasciola hepatica develop a type 2 immune response and concomitant suppression of leukocyte proliferation. *Infect. Immun.* **86** (2018).
- Rodriguez, E. et al. Glycans from fasciola hepatica modulate the host immune response and TLR-Induced maturation of dendritic cells. *PLoS Negl. Trop. Dis.* **9**, e0004234 (2015).
- Howell, A. K., McCann, C. M., Wickstead, F. & Williams, D. J. L. Co-infection of cattle with fasciola hepatica or *F. gigantica* and *Mycobacterium bovis*: A systematic review. *PLoS One* **14**, e0226300 (2019).
- Brown, W. C., Davis, W. C., Dobbelaere, D. A. & Rice-Ficht, A. C. CD4+ T-cell clones obtained from cattle chronically infected with fasciola hepatica and specific for adult worm antigen express both unrestricted and Th2 cytokine profiles. *Infect. Immun.* **62**, 818–827 (1994).
- Perez-Caballero, R. et al. Comparative dynamics of peritoneal cell immunophenotypes in sheep during the early and late stages of the infection with fasciola hepatica by flow cytometric analysis. *Parasites Vectors* **11**, 640 (2018).
- Hidalgo, C., Stoores, C., Hernandez, M. & Paredes, R. Fasciola hepatica coinfection modifies the morphological and immunological features of *Echinococcus granulosus* cysts in cattle. *Vet. Res.* **51**, 76 (2020).
- Petrone, L. et al. Evaluation of the local and peripheral immune responses in patients with cystic echinococcosis. *Pathogens* **13** (2024).
- Hamad, B. S., Shnawa, B. H., Alrawi, R. A. & Ahmed, M. H. Comparative analysis of host immune responses to hydatid cyst in human and ovine hepatic cystic echinococcosis. *Vet. Immunol. Immunopathol.* **273**, 110775 (2024).
- Sweed, D. et al. Does the expression of granzyme B participate in inflammation, fibrosis, and fertility of hydatid cysts? *Parasitol. Res.* **123**, 22 (2023).
- De Prisco, B. D. et al. Evaluation of the local immune response to hydatid cysts in sheep liver. *Vet. Sci.* **10** (2023).
- Baldwin, C. L. et al. Special features of gammadelta T cells in ruminants. *Mol. Immunol.* **134**, 161–169 (2021).
- Hidalgo, C. et al. Response patterns in adventitial layer of *Echinococcus granulosus sensu stricto* cysts from naturally infected cattle and sheep. *Vet. Res.* **52**, 66 (2021).
- Smith, F. et al. Localization of T and B lymphocytes in histologically normal adult human donor liver. *Hepatogastroenterology* **50**, 1311–1315 (2003).
- Correa, F. et al. Cattle co-infection of *Echinococcus granulosus* and fasciola hepatica results in a different systemic cytokine profile than single parasite infection. *PLoS One* **15**, e0238909 (2020).
- Jiménez, M. et al. Fasciola hepatica co-infection enhances Th1 immune response in the adventitial layer of non-fertile *Echinococcus granulosus* cysts. *Vet. Parasitol.* **290**, 109343 (2021).
- Baldwin, C. L. et al. Special features of  $\gamma\delta$  T cells in ruminants. *Mol. Immunol.* **134**, 161–169 (2021).
- Plattner, B. L., Doyle, R. T. & Hostetter, J. M. Gamma-delta T cell subsets are differentially associated with granuloma development and organization in a bovine model of mycobacterial disease. *Int. J. Exp. Pathol.* **90**, 587–597 (2009).

43. Palmer, M. V., Waters, W. R. & Thacker, T. C. Lesion development and immunohistochemical changes in granulomas from cattle experimentally infected with *Mycobacterium bovis*. *Vet. Pathol.* **44**, 863–874 (2007).
44. Howell, A. K. & Williams, D. J. L. The epidemiology and control of liver flukes in cattle and sheep. *Vet. Clin. Food Anim. Pract.* **36**, 109–123 (2020).
45. Stuenkel, S. & Ersdal, C. Fasciolosis—An increasing challenge in the sheep industry. *Animals* **12**, 1491 (2022).
46. Pérez, J. et al. Immunohistochemical study of the local immune response to fasciola hepatica in primarily and secondarily infected goats. *Vet. Immunol. Immunopathol.* **64**, 337–348 (1998).
47. Meeusen, E., Lee, C. S., Rickard, M. D. & Brandon, M. R. Cellular responses during liver fluke infection in sheep and its evasion by the parasite. *Parasite Immunol.* **17**, 37–45 (1995).
48. McCole, D. F., Doherty, M. L., Baird, A. W., Davies, W. C., McGill, K. & Torgerson P.R. T cell subset involvement in immune responses to *Fasciola hepatica* infection in cattle. *Parasite Immunol.* **21**, 1–8 (1999).
49. Sun, Y. et al. Sudan black B reduces autofluorescence in murine renal tissue. *Arch. Pathol. Lab. Med.* **135**, 1335–1342 (2011).
50. McGill, J. L. et al. Specific recognition of mycobacterial protein and peptide antigens by  $\gamma\delta$  T cell subsets following infection with virulent *Mycobacterium bovis*. *J. Immunol.* **192**, 2756–2769 (2014).

## Acknowledgements

The authors would like to thank the staff of “Servicio Agrícola y Ganadero” (SAG) for their support and assistance in collecting *E. granulosus sensu lato* cysts and *F. hepatica* infected liver samples at abattoirs. This work was funded by ANID-Fondecyt Grant #1231620.

## Author contributions

C.S. performed all of the experiments, data analysis and wrote the manuscript first draft; M.S.B. assisted in sample obtainment and provided technical assistance with sample processing; C.H. assisted in sample obtainment and writing-revising the manuscript; C.C.V. performed formal data analysis and provided technical assistance; R.P. validated the experimental design, reviewed obtained data, managed project resources and revised the manuscript. All authors read and approved the final manuscript.

## Declarations

### Competing interests

The authors declare no competing interests.

### Additional information

**Supplementary Information** The online version contains supplementary material available at <https://doi.org/10.1038/s41598-025-95690-8>.

**Correspondence** and requests for materials should be addressed to R.P.

**Reprints and permissions information** is available at [www.nature.com/reprints](http://www.nature.com/reprints).

**Publisher’s note** Springer Nature remains neutral with regard to jurisdictional claims in published maps and institutional affiliations.

**Open Access** This article is licensed under a Creative Commons Attribution-NonCommercial-NoDerivatives 4.0 International License, which permits any non-commercial use, sharing, distribution and reproduction in any medium or format, as long as you give appropriate credit to the original author(s) and the source, provide a link to the Creative Commons licence, and indicate if you modified the licensed material. You do not have permission under this licence to share adapted material derived from this article or parts of it. The images or other third party material in this article are included in the article’s Creative Commons licence, unless indicated otherwise in a credit line to the material. If material is not included in the article’s Creative Commons licence and your intended use is not permitted by statutory regulation or exceeds the permitted use, you will need to obtain permission directly from the copyright holder. To view a copy of this licence, visit <http://creativecommons.org/licenses/by-nc-nd/4.0/>.

© The Author(s) 2025